

Copyright Notice

©ACM, (2006). This is the author's version of the work. It is posted here by permission of ACM for your personal use. Not for redistribution. The definitive version was published in Proc. ACM MSWiM, Torremolinos, Malaga, Spain (October 2006)
<http://doi.acm.org/10.1145/nnnnnn.nnnnnn>

Towards Frequency Reuse 1 Cellular FDM/TDM Systems

Marc C. Necker

Institute of Communication Networks and Computer Engineering
University of Stuttgart, Pfaffenwaldring 47, D-70569 Stuttgart, Germany

Email: marc.necker@ikr.uni-stuttgart.de

ABSTRACT

Classical FDM/TDM cellular networks, such as GSM, avoid the reuse of the same set of frequencies in close-by cells. This is necessary in order to keep the interference level in the cells below a certain threshold. As a drawback, each cell only uses a fraction of the total frequency resources. Eventually, it would be desirable to fully utilize the complete available frequency spectrum in each cell. In this paper, we demonstrate how beamforming antennas in combination with an intelligent interference coordination in-between cells can be used to achieve this goal. We investigate the tradeoff between the achievable Signal-to-Interference Ratio (SIR) in each cell and the effective utilization of the frequency resources at the example of a state-of-the-art 802.16e system. We conclude that the investigated mechanisms open the way to future wireless access networks with an efficient utilization of the available frequency spectrum.

Categories and Subject Descriptors

H.m [Information Systems]: Miscellaneous

General Terms

Algorithms, Performance

Keywords

WiMax, 802.16e, interference coordination, FDM, TDM, OFDMA, beamforming antennas

1. INTRODUCTION

With the development of high speed wireless access networks, frequency spectrum has become the most precious resource. State-of-the-art wireless systems apply advanced mechanisms on the physical layer in order to push throughput performance. Most prominent examples are Adaptive Modulation and Coding schemes [7, 6] and Hybrid Automatic Repeat Request (HARQ) mechanisms [4]. Additionally, fast channel-aware scheduling mechanisms can provide

a significant increase in system capacity by exploiting multi-user diversity [11, 14].

Despite those efforts, the system capacity remains limited by many factors. In broadband cellular access networks, one of the main limitations is the interference that a transmission in one cell causes to other cells. This limits the achievable Signal-to-Interference Ratio (SIR) and hence the achievable throughput especially in the border areas of a cell. CDMA-based systems, such as High Speed Downlink Packet Access (HSDPA), try to solve this issue by spreading and the usage of different scrambling codes in adjacent cells. In contrast, classical FDM-based systems, such as GSM, must avoid the reuse of the same frequency range in cells within a certain area. This limits the utilization of the available frequency spectrum, which is captured in the frequency reuse factor. A frequency reuse factor of 3 indicates a utilization of 1/3 of the available frequency spectrum, where most operational systems need to apply even higher frequency reuse factors in order to achieve full coverage. Ideally, the frequency reuse factor should be 1 while still maintaining acceptable SIR-conditions even at the cell borders.

In the past years, smart antenna systems have gained growing attention as an attractive way of increasing the throughput of wireless systems. A lot of research has focused on diversity Multiple-Input-Multiple-Output (MIMO) systems which base their throughput increase on the availability of multiple uncorrelated channels in-between the elements of the transmitter's and receiver's smart antenna systems. Another alternative is to use beamforming algorithms in order to steer the main lobe of the smart antenna system towards the receiving terminal, thus increasing the received signal level. At the same time, this reduces the interference caused to neighboring cells, allowing for a better frequency reuse. In advanced beamforming systems, the mobile terminal can be tracked with an angular accuracy of a few degrees [12].

Simpler versions are switched beam systems. They apply a limited number of fixed beams, which are activated depending on the mobile terminal's position. A comparable system with 4 switched beams per 120° cell sector is studied in [2] at the example of a GSM/EDGE Radio Access Network (GERAN). Using both simulations and drive test measurements the authors achieved an SIR gain of 3-4dB compared to regular sector antennas. A more fundamental study of switched beam smart antennas in cellular networks can be found in [8].

Another approach to limit the interference is the coordination of transmitting nodes in the network, also known

Permission to make digital or hard copies of all or part of this work for personal or classroom use is granted without fee provided that copies are not made or distributed for profit or commercial advantage and that copies bear this notice and the full citation on the first page. To copy otherwise, to republish, to post on servers or to redistribute to lists, requires prior specific permission and/or a fee.

MSWiM'06, October 2-6, 2006, Torremolinos, Malaga, Spain.

Copyright 2006 ACM 1-59593-477-4/06/0010 ...\$5.00.

as interference coordination. In [10], the coordination of transmissions in a multi-hop wireless network is considered. The interference conditions are evaluated on a fine granular time-scale, and an omnipotent central entity with full system state information is assumed to be able to schedule the data transmissions of the individual nodes on the MAC-frame level. In [16], the authors consider the possibility of beamforming in a similar scenario. They first evaluate the general improvement with respect to the interference conditions compared to omnidirectional antennas. Subsequently, they study the requirements for a MAC protocol, which is capable of blocking the transmissions of the strongest interferers.

In cellular systems, interference coordination among base-stations has gained little attention so far. In [15], the possibility of coordinating the transmissions in adjacent cell sectors, which are served by the same base-station, is considered. This allows a frequency reuse factor of 1 close to the base-station, and a higher frequency reuse factor only in the outer regions of the cell. Altogether, the authors achieve an effective frequency reuse of 1.5–2 with an average SIR of 16dB within the cell. The realization of the basic concept is relatively easy, since no signaling among base-stations is required.

The case of inter-cellular coordination in order to reduce interference is studied in [3] and [13]. In both papers, the authors focus on a flow-level analysis of the possible capacity gains with inter-cellular coordination in some basic scenarios. They derive the optimal boundaries of regions which may or may not be served by the same base-stations at the same time, resulting in a static scheduling policy for each cell. The case of beamforming to reduce interference by spatial separation of transmissions is not directly taken into account.

In our paper, we investigate the benefits of inter-cellular coordination at the frame-level in a fully dynamic scenario. We explicitly take into account the capability of beamforming antennas to spatially separate transmissions in neighboring cells in order to limit interference. Similar to the approach in [10], we assume that a central entity with full system-state information is capable of performing dynamic

scheduling decisions for all base-stations on a MAC-frame level. This allows us to evaluate the ideally achievable performance of the system, which is an important reference for future realistic and implementable algorithms. In particular, we study how the transmissions of all base-stations can be coordinated such that a minimum desired SIR is achieved throughout the network area. We quantify how an increase in SIR reduces the utilization of transmission resources, corresponding to an increase of the effective frequency reuse factor. This lower resource utilization is counteracted by higher data rates available at higher SIR values. Therefore, we also investigate the average sector throughput in order to evaluate the trade-off between the resource utilization and the SIR level and obtain the optimal operating point.

This paper is structured as follows: In section 2, we introduce the underlying 802.16e system and the considered scenario. In section 3, we detail the interference coordination algorithm. The performance of the interference coordinated system is subsequently evaluated in section 4 together with uncoordinated frequency reuse 3 and 1 reference systems. Finally, section 5 concludes the paper.

2. SYSTEM MODEL

2.1 Overview of transmission system

As an example of an FDM/TDM based access network, we will use an 802.16e-system [9] in the Orthogonal Frequency Division Multiple Access (OFDMA) mode. The total available system bandwidth is set to 10 MHz with a MAC-frame-length of 5 ms. This results in a total number of 49 OFDM-symbols per MAC-frame and 768 data subcarriers per OFDM-symbol. Each MAC-frame is subdivided into an uplink and a downlink subframe. Both subframes are further subdivided into zones, allowing for different operational modes. In this paper, we will focus on the Adaptive Modulation and Coding (AMC) zone in the downlink subframe. In particular, we focus on the AMC 2x3 mode, which defines subchannels of 16 data subcarriers by 3 OFDM-symbols. This is illustrated in the left part of Fig. 1. A subchannel corresponds to the resource assignment granularity for a particular mobile terminal. The AMC zone can therefore be abstracted by the two-dimensional resource field shown in the right part of Fig. 1.

For our performance evaluation, we assume the AMC zone to consist of 9 OFDM-symbols, corresponding to a total number of $48 \cdot 3$ available subchannels. Adaptive Modulation and Coding was applied ranging from QPSK 1/2 up to 64QAM 3/4. This results in a theoretical maximum data rate of about 6.2 Mbps within the AMC zone.

2.2 Simulation model

We consider a hexagonal cell layout comprising 19 base-stations with 120° cell sectors as shown in Fig. 2. Throughout our paper, we evaluate the shaded *observation area* when investigating the cell coverage, and the marked reference cell sectors for sector specific results. All cells were assumed to be synchronized on a frame level. Each sector contains N fully mobile terminals, which are restricted to their respective cell sector in order to avoid handovers.

Base-stations are located at the center of the hexagons with one transceiver per cell sector. Depending on the scenario, the transceivers are equipped with sector antennas or beamforming antennas. The gain patterns of both an-

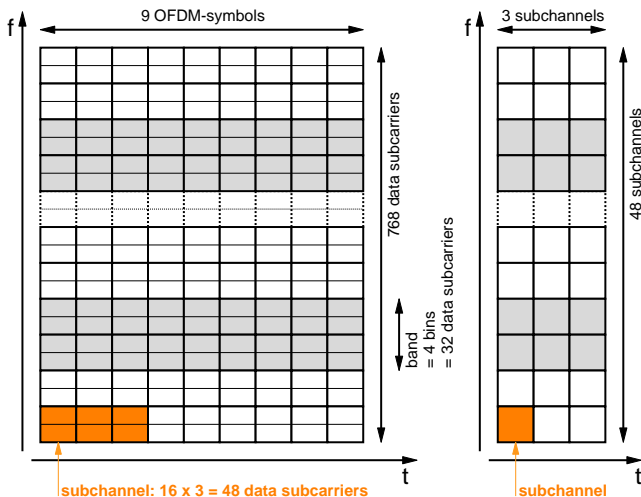


Figure 1: Illustration of the AMC 2x3 mode

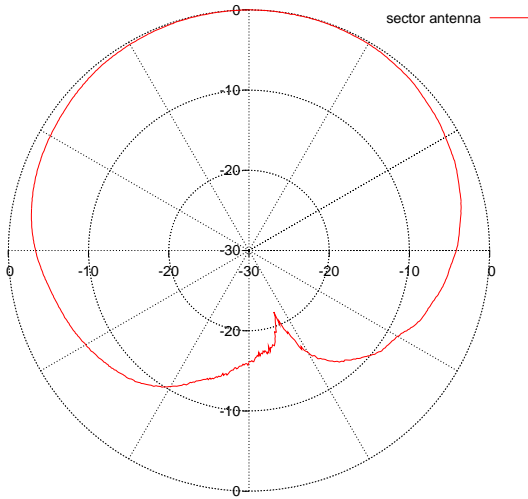


Figure 3: Sector antenna beam pattern, normalized to gain in main lobe direction of 0°

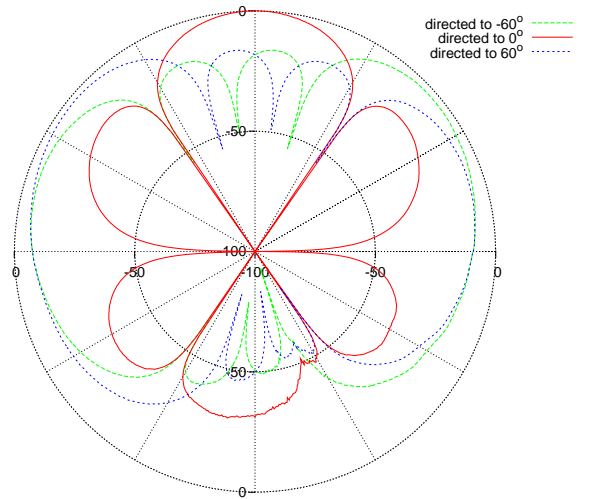


Figure 4: 4-element array beam patterns for three different steering directions, normalized to maximum gain in main lobe direction when steered towards 0°

Antenna configurations are plotted in Fig. 3 and 4, respectively, where the main lobe direction is towards the top of the diagrams. For the beamforming antenna, the gain patterns for three different steering directions are shown as examples, namely for the sector borders ($\pm 60^\circ$) and the sector center (0°). Note that the beamforming antenna has an additional beamforming gain of about 4.5 dBi.

The beamforming antennas can be steered towards each terminal with an accuracy of 1° degree. At the same time we assume that all terminals can be tracked ideally. Consequently, in the scenarios with beamforming antennas, the

antennas are always directed towards the mobiles they are currently transmitting to.

3. INTERFERENCE COORDINATION AND RESOURCE ASSIGNMENT

3.1 General procedure

As illustrated in Fig. 1, each sector has its own set of resources, which need to be assigned to the terminals. This is done on a per-frame basis by a global scheduler. In order to realize the coordination of cell sectors, we divide the scheduling process into two parts per MAC frame:

1. *Creation of an interference graph:* In this step, a graph is created based on the interference relations in-between all mobiles. In this graph, the nodes represent the mobile terminals, and the edges represent critical interference relations in-between the terminals. In particular, terminals which are connected must not be served using the same set of resources. Figure 5 shows an example of an interference graph.

This interference graph is similar to the conflict graph used in [10] regarding its semantics. However, in our case, terminals are only receiving but not transmitting any data.

2. *Resource assignment:* In this second step, a global scheduler assigns resources to the different terminals, while taking into account the constraints of the interference graph.

Both steps are performed for each MAC frame. This implies that there is an omniscient device capable of instantly acquiring the system state and assigning the resources on a per-frame basis. This is an ideal solution, which is not feasible in an actual system. A realizable solution will need

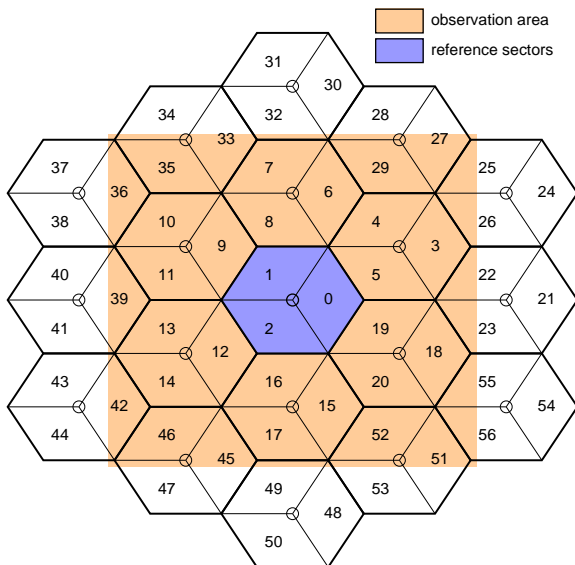


Figure 2: Hexagonal cell layout

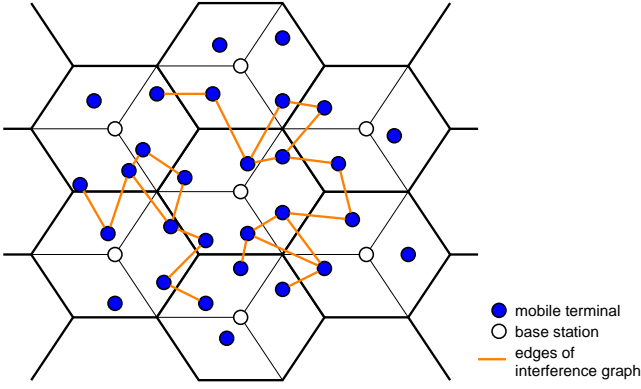


Figure 5: Example of interference graph

to be able to cope with signaling delays and limited system state information. However, the idealized procedure described above delivers an upper performance bound, which is essential to evaluate any realizable solution. It also allows us to assess the fundamental performance limits of a frequency reuse 1 system.

The creation of the interference graph is detailed in the following section 3.2, and the subsequent step of resource assignment in section 3.3.

3.2 Construction of interference graph

We construct the interference graph by evaluating the interference that a transmission to one mobile terminal causes to any other terminal. For each terminal, we first calculate the total interference and then block the largest interferers from using the same set of resources by establishing a relation in the graph. This is done such that a desired minimum SIR D_S is achieved.

Let m_k and m_l be two mobile terminals in different cell sectors, as illustrated in Fig. 6. tr_i denotes the transceiver serving cell sector i . p_{ik} describes the path loss from transceiver tr_i to terminal m_k , including shadowing. We further introduce the function $G_i(l, k)$. It describes the gain of the sector i beamforming antenna towards terminal m_k when the array is directed towards terminal m_l . $e_{kl} \in \{0, 1\}$ are the elements of the interference graph's adjacency matrix E , indicating an interference relation between terminals m_k and m_l if $e_{kl} = 1$.

In a first step, we calculate the interference I_{kl} which a transmission to mobile m_l in sector i would cause to mobile m_k in sector j , where $i \neq j$:

$$I_{kl} = p_{ik} G_i(l, k) P_l, \quad (1)$$

where P_l is the transmission power of transceiver i towards terminal m_l . For each terminal m_k , we collect all interference relations in the set W_k :

$$W_k = \{I_{kl}, \forall l \neq k\}. \quad (2)$$

We then keep removing the largest interferer from W_k until the worst-case SIR for terminal m_k rises above a given desired SIR threshold D_S :

$$\text{SIR}_k = \frac{S_k}{\sum_{I_{kl} \in W_k} I_{kl}} \geq D_S. \quad (3)$$

S_k is the received signal strength of terminal m_k if it is served:

$$S_k = p_{jk} G_j(k, k) P_k. \quad (4)$$

The edges e_{kl} of the interference graph then follow as:

$$e_{kl} = \begin{cases} 0 & \text{if } I_{kl} \in W_k \wedge I_{lk} \in W_l \\ 1 & \text{otherwise} \end{cases}. \quad (5)$$

Equation (5) sets an interference relation e_{kl} if terminal m_k causes interference to terminal m_l , or vice versa. This is necessary since in both cases the usage of the same set of resources must be avoided. This results in a unidirectional interference graph, i.e., E is symmetric.

3.3 Resource assignment

In each cell sector, a Round Robin (RR) scheduling mechanism is used to determine the scheduling order of the terminals. The RR scheduler rotates the scheduling order among all N terminals within a cell such that every terminal is assigned the highest scheduling priority exactly once every N MAC-frames. The terminal with the highest priority in frame n becomes the mobile with the second highest priority in frame $n + 1$, and so on.

For each MAC frame, the resource assignment process then begins by randomly selecting a cell sector and assigning a rectangle of 3×12 subchannels in the two-dimensional time/frequency plane to the highest priority terminal m_k . The assigned resources are then blocked for all other terminals connected to m_k in the interference graph. Afterwards, another cell sector is randomly selected and the highest priority terminal is assigned resources, obeying possible resource blockings. Once all sectors have been visited, the whole procedure is repeated with the second highest priority terminals, and so on. The resource assignment process is completed if all resources in all sectors have been assigned, or if no more assignments are possible due to conflicts in the interference graph.

4. PERFORMANCE EVALUATION

4.1 Overview

In this section, we evaluate the system performance with respect to the cell coverage, the utilization of the cell sector

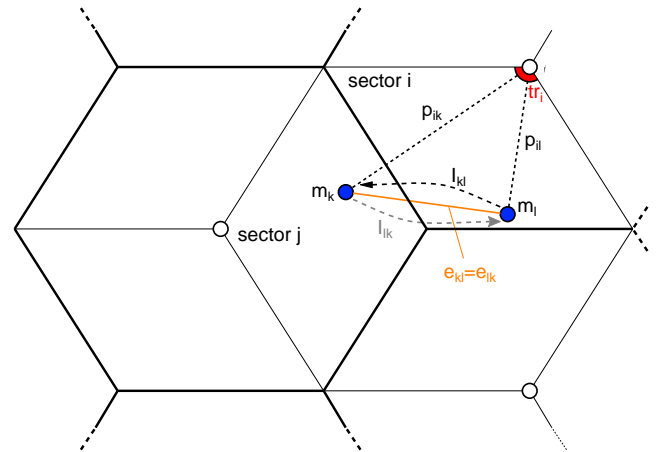


Figure 6: Creation of the interference graph

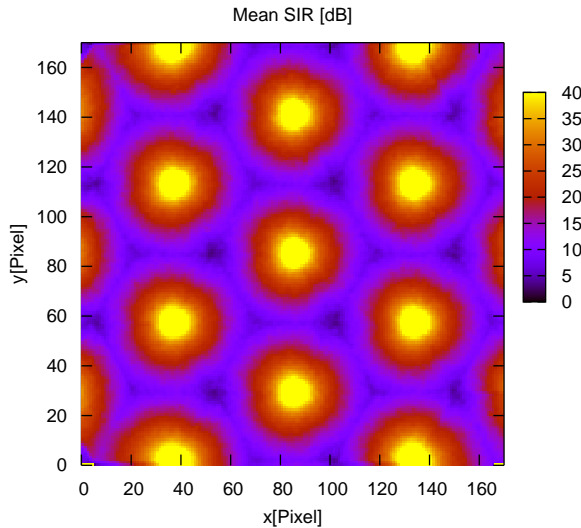


Figure 7: Mean SIR, 120° sector antennas, frequency reuse 3

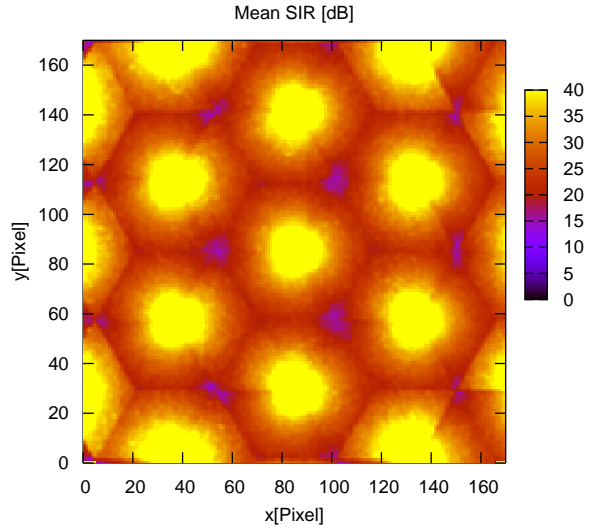


Figure 8: Mean SIR, beamforming antennas, frequency reuse 3

resources, and the overall throughput. After the presentation of the simulation parameters in section 4.2, we first investigate the cell coverage of a frequency reuse 3 system in section 4.3 in order to obtain reference performance values. We then detail the performance of a frequency reuse 1 system by analyzing the cell coverage without interference coordination in section 4.4, and by studying the coverage gain achieved by the interference coordination process in section 4.5. Finally, we investigate the utilization of the cell sector resources and the overall sector throughput in section 4.6.

4.2 Scenario and simulation parameters

The system model was implemented as a frame-level simulator using the event-driven simulation library IKR SimLib [1]. The distance between two basestations was set to 1,400 m. The path loss was modeled according to [5], terrain category B. Slow fading was considered using a log-normal shadowing model with a standard deviation of 8 dB. Frame errors were modeled based on BLER-curves obtained from physical layer simulations considering both ARQ and HARQ with chase combining.

Each sector contains N mobile terminals moving at a velocity of $v = 30$ km/h. The underlying mobility model is a random direction model with a mean free path length of 50 m and a maximum turning angle of 25° . As all mobile terminals are bound to their respective cell sector, they are reflected at the sector borders if they were to leave the sector. A greedy traffic source is transmitting data towards each terminal, i.e., there is always data available to be transmitted for a terminal.

4.3 Performance of uncoordinated frequency reuse 3 system

Figure 7 plots the mean SIR over the observation area defined in Fig. 2 for the case of a frequency reuse 3 system with sector antennas. In this scenario, $1/3$ of the frequency resources are available in each cell sector, and the downlink transmissions are not coordinated in-between the sectors.

The yellow areas in Fig. 7 indicate areas with a mean SIR of 40 dB or more. As the individual sectors of a basestation do not cause any interference to each other in a frequency reuse 3 system, we can observe excellent SIR conditions close to the basestations. In the border areas of the cells, the mean SIR is too low to guarantee acceptable system performance. However, we should note that the presented results are only average values of the SIR. The instantaneous SIR may be much higher or much lower, depending on the particular interference condition and scheduling decision in each MAC frame. The communication with terminals in the border areas could possibly still be maintained, since the instantaneous SIR may sometimes be much higher.

Figure 9 supplements these results by plotting the 5% quantile of the SIR in the observation area. In the black areas, the SIR is below 0 dB in more than 5% of all transmissions. This picture illustrates the relatively poor SIR performance of a frequency reuse 3 system when considering that it aims at supporting broadband services.

In the next step, we substitute the sector antennas by beamforming antennas. Upon each transmission, the beam is directed towards the respective mobile terminal, thus reducing the interference in neighboring cell sectors. The system still operates with a frequency reuse of 3 and no interference coordination in-between sectors. For this configuration, Fig. 8 plots the mean SIR in the observation area. Compared to the case of sector antennas in Fig. 7, the mean SIR is significantly higher. Even in the border areas of the cells, we achieve good average SIR performance. Nevertheless, the 5% quantile shown in Fig. 10 still shows large areas where the instantaneous SIR drops below an acceptable threshold.

4.4 Performance of uncoordinated frequency reuse 1 system

In a frequency reuse 1 system, the usage of the complete available frequency spectrum is allowed in all cell sectors. Figure 11 plots the mean SIR over the observation area with sector antennas and no interference coordination. This leads

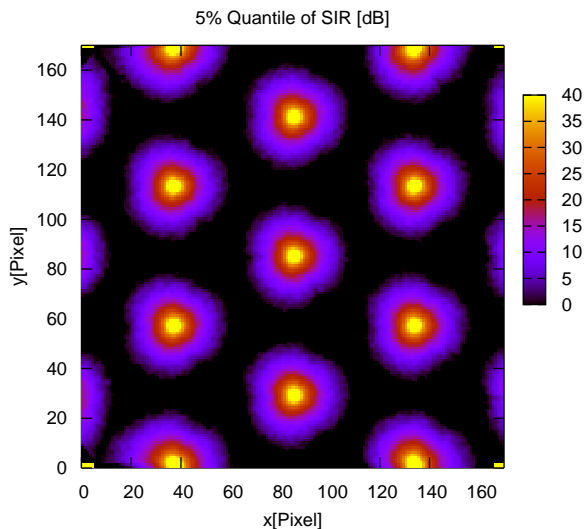


Figure 9: 5% quantile of SIR, 120° sector antennas, frequency reuse 3

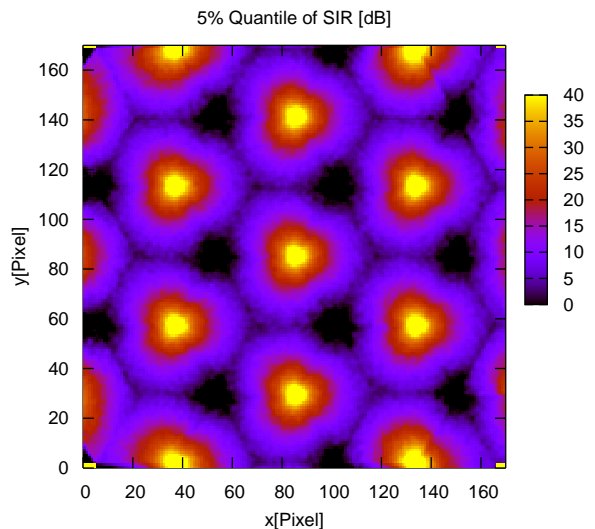


Figure 10: 5% quantile of SIR, beamforming antennas, frequency reuse 3

to severe other-cell interference conditions. The black areas indicate regions with an SIR of 0 dB or lower. As expected, there is hardly any region with a mean SIR sufficient for a regular system operation.

When replacing the sector antennas with beamforming antennas, we obtain a significantly better mean SIR in large areas, as can be seen in Fig. 12. Critical regions are still the border areas of the cells, especially at the three-cell contact points. However, regular system operation would be possible in about half of the investigated area, though with reduced data rates.

4.5 Performance of interference coordinated frequency reuse 1 system

In this section, we extend the scenario by the interference coordination functionality described in section 3. The average SIR in the observation area for the two scenarios with sector antennas and beamforming antennas are shown in Fig. 13 and 14, respectively, for a minimum desired SIR of $D_S = 15$ dB. In both cases, the observed mean SIR is significantly higher than in the uncoordinated system and also much higher than the desired minimum SIR D_S . This is simply because D_S refers to the worst-case SIR, and the actually achieved SIR will often be better. The 5% quantile of the SIR is not plotted here. It is almost constant throughout the observation area, except for small areas very close to the basestations. In the case of sector antennas, it is around 27–28 dB, and around 23–24 dB in the case of beamforming antennas. This is yet another indication that D_S only describes the minimum SIR.

Both the mean SIR and the quantile attest the sector antennas a slightly better coverage. This is due to the higher number of interference relations in the interference graph compared to the beamforming case. Consequently, it is more difficult to assign all available resources during the resource assignment step. This leads to a lower utilization of the available resources, which counteracts the increased

data rates that higher SIR values allow. We detail this effect in section 4.6.

The SIR conditions in the reference sectors are further illustrated in Fig. 15. The chart plots the median and the 1% quantile of the SIR values experienced by the terminals depending on the desired minimum SIR D_S . Note that we need to evaluate the median since the mean is dominated by high SIR values of those terminals which are close to the basestation. Shown are the curves for the beamforming and the sector antenna case and for two different number of mobiles N . In all cases, the median and the quantile exhibit a linear relation to the desired SIR D_S . Both the median and the quantile of the SIR indicate better conditions in the case of sector antennas, which supports the previous results in Fig. 13 and 14. When increasing the number of terminals, we observe an increase in the SIR performance, which can be traced back to the greater flexibility during the resource assignment step and the slightly lower resource utilization (see section 4.6).

4.6 Effective frequency reuse and sector throughput

In a frequency reuse 1 system, the utilization of the resources is 100%, whereas in a frequency reuse three system the utilization is fixed to $1/3$. The resource utilization is therefore directly related to the effective frequency reuse factor achieved by the system. In our case, the resource utilization dynamically results from the interference graph and the subsequent resource assignment step. As we increase the desired minimum SIR D_S , it becomes more difficult to assign all available resources. This is due to the increased number of conflicts in the interference graph. Consequently, the increased SIR performance observed in the previous section comes at the price of a lower utilization of the individual cell sector's resources. Again, this counteracts the higher data rates that come along with the higher SIR values.

This increase of the effective frequency reuse factor is illustrated in Fig. 16, which shows the mean utilization of the

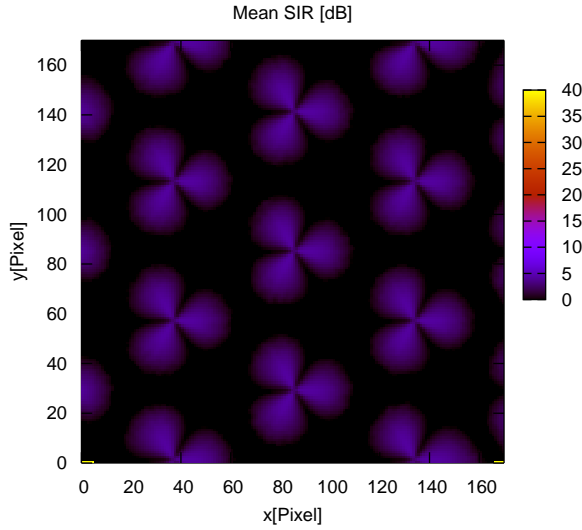


Figure 11: Mean SIR, 120° sector antennas, no interference coordination

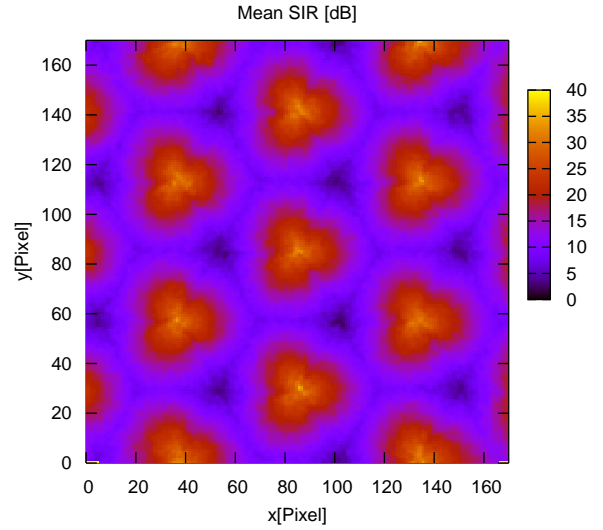


Figure 12: Mean SIR, beamforming antennas, no interference coordination

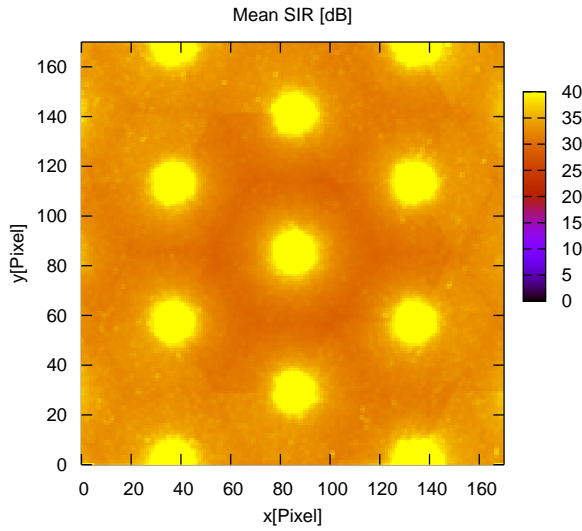


Figure 13: Mean SIR, 120° sector antennas, interference coordination with $D_S = 15$ dB

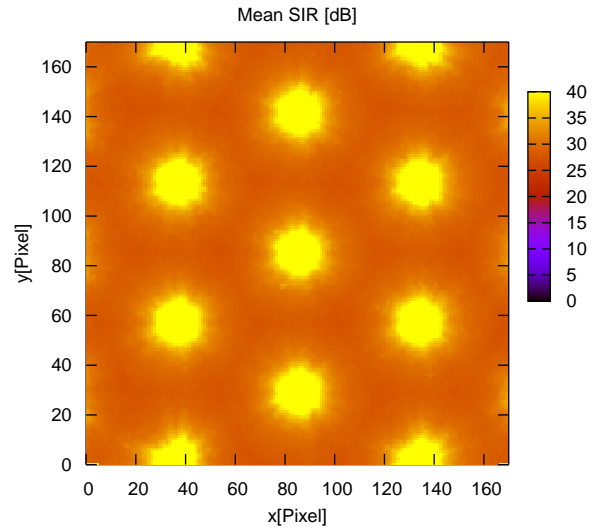


Figure 14: Mean SIR, beamforming antennas, interference coordination with $D_S = 15$ dB

resources in the reference sectors over the desired SIR D_S . As expected, the utilization decreases as D_S is increased. The graph also reveals the significantly lower resource utilization in the case of sector antennas already explained in section 4.5. When increasing the number of mobiles N per cell sector from 9 to 15, the resource utilization shows a slight decrease. The reason is the more complicated resource assignment process when more mobiles need to be considered.

An increased SIR allows for higher data rates due to the application of adaptive modulation and coding schemes. A better SIR therefore has the potential to compensate the effect of a lower resource utilization. Figure 17 takes into account both effects by plotting the average sector throughput

over D_S . When first looking at the results in the beamforming scenario, we can observe a maximum for the throughput at a minimum SIR of $D_S \approx 10 - 15$ dB for the beamforming case, and $D_S \approx 5 - 10$ dB for the case of sector antennas. At these points, the SIR conditions are optimally traded off against the resource utilization in the considered scenario. We also observe a considerable gain as we increase the number of mobiles N in the beamforming case, resulting from the improved SIR conditions as detailed before. Compared to the case of sector antennas, the beamforming antennas can achieve an approximately three times as large average sector throughput.

Finally, we compare these results to those of the uncoordinated frequency reuse 3 system from section 4.3. With

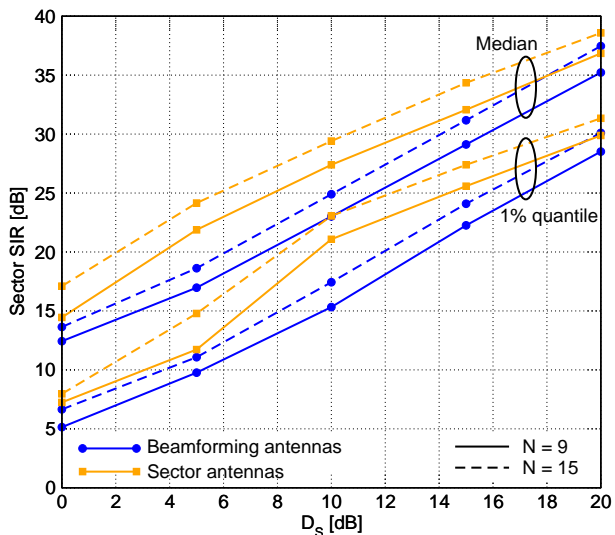


Figure 15: Median and 1% quantile of SIR in reference sectors

sector antennas and $N = 9$, the average sector throughput of the frequency reuse 3 system is about 634 kbps. Compared to the throughput achieved by the interference coordinated system in Fig. 17, this is an approximately 4% higher throughput. This results from the low utilization of resources in the sector antenna case, as observed in Fig. 16. However, we need to note that the coverage of the reuse 3 system is much worse than the coverage of the interference coordinated system.

When moving to beamforming antennas, the average sector throughput of the frequency reuse 3 system increases to about 1245 kbps. This means that the interference coordinated frequency reuse 1 system with beamforming antennas achieves a throughput which is about 54% higher compared to a similar frequency reuse 3 system, and an about 3 times

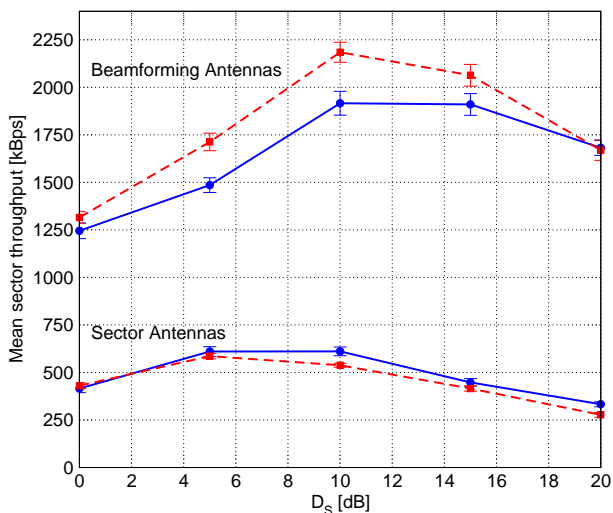


Figure 17: Mean throughput in reference sectors

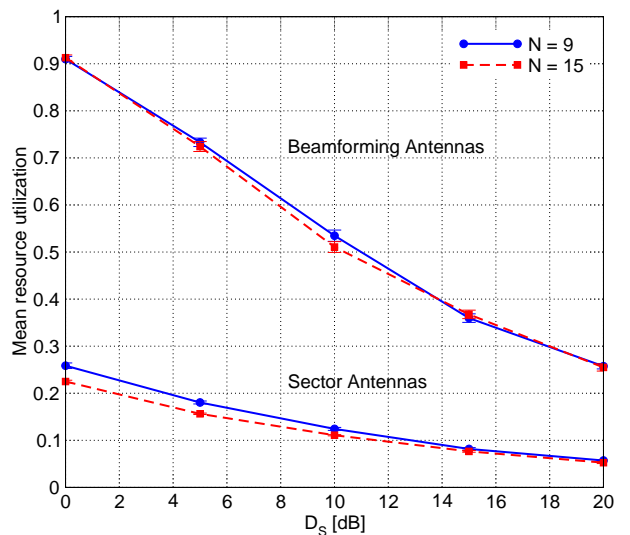


Figure 16: Mean utilization of resources in reference sectors

higher throughput than a frequency reuse 3 system with sector antennas.

5. CONCLUSION

We compared the coverage and throughput performance of a frequency reuse 3 and a frequency reuse 1 cellular FDM system in the absence and presence of interference coordination in-between cells. In all investigated scenarios, the application of beamforming antennas significantly improves the throughput performance. The uncoordinated frequency reuse 3 system achieves acceptable performance in most regions. However, it shows a significant degradation in the cell border areas, especially with respect to the instantaneous SIR. In contrast, a coordinated frequency reuse 1 system can maintain a minimum required SIR in all of the area. We illustrated the trade-off between the minimum SIR and the utilization of the available frequency spectrum, leading to an optimum of the average sector throughput for a particular minimum SIR. We finally demonstrated that a coordinated frequency reuse 1 system with beamforming antennas can outperform a classical frequency reuse 3 system by a factor of about 1.6 with respect to the utilization of frequency resources and a factor of about 1.5 with respect to the average sector throughput.

6. ACKNOWLEDGMENTS

This research was done in cooperation with Alcatel Research and Innovation Department, Stuttgart.¹ The author would like to thank Christoph Gauger, Detlef Saß, Andreas Weber, and Bozo Cesar for their valuable input and discussions.

¹Alcatel SEL AG, Research & Innovation, Lorenzstr. 10, 70435 Stuttgart, Germany. Contact: Roland Münzner (Roland.Muenzner@alcatel.de).

7. REFERENCES

- [1] IKR simulation library. <http://www.ikr.uni-stuttgart.de/Content/IKRSimLib/>.
- [2] C. Ball, K. Ivanov, H. Winkler, M. Westall, and E. Craney. Performance analysis of a GERAN switched beam system by simulations and measurements. In *Proc. 59th IEEE Vehicular Technology Conference (VTC 2004-Spring)*, volume 1, pages 88–92, May 2004.
- [3] T. Bonald, S. Borst, and A. Proutière. Inter-cell scheduling in wireless data networks. In *Proc. European Wireless (EW 2005)*, Nicosia, Cyprus, 2005.
- [4] R. A. Comroe and D. J. Costello, Jr. ARQ schemes for data transmission in mobile radio systems. *IEEE Journal on Selected Areas in Communications*, 2(4):472–481, July 1984.
- [5] V. Erceg, L. Greenstein, S. Tjandra, S. Parkoff, A. Gupta, B. Kulic, A. Julius, and R. Bianchi. An empirically based path loss model for wireless channels in suburban environments. *IEEE Journal on Selected Areas in Communications*, 17(7):1205–1211, July 1999.
- [6] A. Goldsmith and S.-G. Chua. Variable-rate variable-power MQAM for fading channels. *IEEE Transactions on Communications*, 45(10):1218–1230, October 1997.
- [7] J. Hayes. Adaptive feedback communications. *IEEE Transactions on Communications*, 16(1):29–34, February 1968.
- [8] M.-J. Ho, G. Stüber, and M. Austin. Performance of switched-beam smart antennas for cellular radiosystems. *IEEE Transactions on Vehicular Technology*, 47(1):10–19, February 1998.
- [9] IEEE 802.16e. *Draft IEEE Standard for Local and metropolitan area networks, Part 16: Air Interface for Fixed Broadband Wireless Access Systems, Amendment for Physical and Medium Access Control Layers for Combined Fixed and Mobile Operation in Licensed Bands*, October 2004.
- [10] K. Jain, J. Padhye, V. N. Padmanabhan, and L. Qiu. Impact of interference on multi-hop wireless network performance. In *Proc. of the 9th annual international conference on Mobile computing and networking*, pages 66–80, San Diego, CA, USA, 2003.
- [11] T. Kolding. Link and system performance aspects of proportional fair scheduling in WCDMA/HSDPA. In *Proc. Vehicular Technology Conference 2003 (VTC 2003-Fall)*, volume 3, pages 1717–1722, October 2003.
- [12] A. Kuchar, M. Taferner, M. Tangemann, C. Hoek, W. Rauscher, M. Strasser, G. Pospischil, and E. Bonek. Real-time smart antenna processing for GSM1800 base station. In *Proc. 49th IEEE Vehicular Technology Conference (VTC 1999-Spring)*, volume 1, pages 664–669, May 1999.
- [13] S. Liu and J. Virtamo. Inter-cell coordination with inhomogeneous traffic distribution. In *Proc. 2nd Conference on Next Generation Internet Design and Engineering (NGI 06)*, Valencia, Spain, April 2006.
- [14] M. C. Necker. A comparison of scheduling mechanisms for service class differentiation in HSDPA networks. *International Journal of Electronics and Communications*, 60(2):136–141, February 2006.
- [15] M. Sternad, T. Ottosson, A. Ahlen, and A. Svensson. Attaining both coverage and high spectral efficiency with adaptive OFDM downlinks. In *Proc. 58th IEEE Vehicular Technology Conference (VTC 2003-Fall)*, volume 4, pages 2486–2490, October 2003.
- [16] R. Vilzmann, C. Bettstetter, and C. Hartmann. On the impact of beamforming on interference in wireless mesh networks. In *Proc. IEEE Workshop on Wireless Mesh Networks*, Santa Clara, CA, USA, September 2005.